SIZING AND PERFORMANCE ANALYSIS OF A MW-CLASS ELECTRIFIED AIRCRAFT PROPULSION (EAP) SYSTEM FOR A PARALLEL HYBRID TURBOPROP CONCEPT

Dahlia Dang-Thy Vu Pham[1], Carl Recine[1], and Ralph H. Jansen[2]

[1]NASA Ames Research Center, Moffett Field, CA, 94035
[2]NASA Glenn Research Center, Cleveland, OH, 44135

Abstract

Aircraft electrification has emerged as a pivotal research and development focus in the 21st century, gaining international momentum as a strategic approach to curtail fuel consumption and emissions in the civil aviation sector. Through the Electrified Powertrain Flight Demonstration (EPFD) project, NASA is collaborating with industry partners to raise the technical readiness, address integration challenges, and gather data for future standards and regulations for Megawatt (MW) class Electrified Aircraft Propulsion (EAP) system demonstrators utilized by regional turboprops or single-aisle commercial transports. With the rapid emergence of novel EAP concepts, current efforts are focused on developing the capabilities to evaluate the impacts of electrification on vehicle-level performance. This requires parametric modeling at the conceptual design stage, using uncertainty propagation techniques to account for the high variability in EAP system architecture. This paper details an integrated approach to parametric variation of multi-MW EAP systems in a large turboprop freighter concept with a parallel hybrid configuration. The primary goal is to assess vehicle-level performance sensitivities, such as range and fuel burn reduction, to variations in electrical system component-level performance metrics, including specific power, efficiency, and energy density, based on near-term EAP technology levels.

Keywords: electrified aircraft propulsion, green aviation, aircraft performance

1. Introduction

Improving the sustainability of flight operations worldwide has been the preeminent long-term aspirational goal (LTAG) of the International Civil Aviation Organization (ICAO) [1]. Over the past decade, Electrified Aircraft Propulsion (EAP) systems have emerged as promising solutions to reducing fuel consumption and CO_2 emissions by opting for battery-electric power sources over conventional aviation fuel [2]. Megawatt-class (MW) hybrid electric powertrain systems are being designed, integrated, developed, and tested for future demonstration on turboprop aircraft platforms for cargo and passenger transport operations under NASA programs [3]. Due to the novelty of these aircraft concepts and the technologies required for EAP system integration, systems-level design space exploration is critical in validating whether benefits such as reducing CO_2 emissions and improving fuel efficiency can be realized by a given concept. Previously, multi-MW electric power system trade-space explorations have been conducted for several single-aisle configurations [4]. Studies conducted by Kirk et al. [5] explored the design space of parallel hybrid aircraft for various sizes and ranges, establishing the complexity and non-intuitive interactions behind component-level parameters and vehicle-level performance metrics for EAP system integrated concepts [5, 6, 7]. Aligning with these developments, the purpose of this study is to model and assess the performance of multi-MW EAP systems through parametric design exploration of component-level metrics such as specific power and efficiency ranges representative of technology levels potentially available within the next ten years [4]. By evaluating the sensitivities between variable EAP system component parameters and overall aircraft performance, this research aims to establish a better understanding of the feasibility and advantages of a parallel hybrid turboprop aircraft for short-haul passenger and cargo operations. This contributes to the broader objective of sustainable aviation and the assessment of MW-class EAP concepts.

2. Concept Overview

While current EAP technology readiness has yet to mature to levels required for the full electrification of single-aisle commercial transports, there is significant potential in the design space for hybridization of short-haul and regional turboprop transports [8, 9]. Since state-of-the-art electrical storage systems maintain significantly lower specific energy densities (approximately 250 Wh/kg pack-level) compared to conventional jet fuel, powertrain electrification impacts vehicle sizing and performance [6]. While many different architectures have been studied and assessed for EAP concepts, the parallel hybrid electric architecture is favored because it directly leverages the improved transmission efficiency of electric machines compared to conventional gas turbines (e.g., ~93% efficiency compared to ~40%) and is also highly configurable [7]. Previous NASA concepts such as PEGASUS and SCEPTOR in Refs. [6, 7] have demonstrated the benefits of parallel hybrid and true parallel hybrid architectures on reduced mission energy consumption for regional turboprop ranges and sizes [9]. Specifically, the true parallel hybrid architecture capitalizes on electrification benefits as it provides the option of maintaining a separate electric propulsion unit (EPU) that is completely independent from the conventional gas turbine propulsor system, which allows for thrust-split optimization across the mission profile [9].

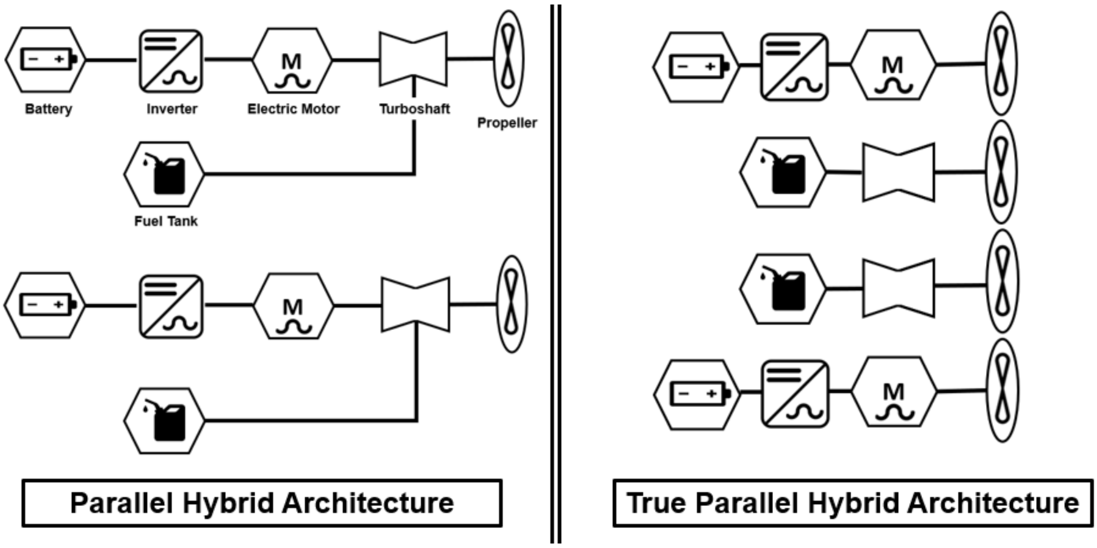

Figure 1. Architecture overview for parallel hybrid and true parallel hybrid EAP systems

Figure 1 shows a comparison of the parallel hybrid and true parallel hybrid electric propulsion architectures and connectivity of the components. Note that there is no mechanical connection between the conventional powertrain and the electric powertrain for the true parallel hybrid architecture. While near-term demonstrations under the EPFD project focus on smaller, regional turboprops with maximum motor power levels ≤1 MW, multi-MW EAP systems are required for large, narrow-body passenger aircraft and single-aisle transports [10]. A notional true parallel hybrid (TPH) large turboprop freighter (LTF) concept was developed to study how variations in component-level performance impacts the performance of a multi-MW hybridized EAP system, in terms of specific power and efficiencies. The TPH LTF is a high-wing, four-propeller turboprop concept with a gross takeoff weight of 150,000 lb that features a dual-sided multi-MW system architecture that utilizes a parallel turbine and electric motor drive system to power the aircraft; the outboard propellers are driven by a pair of multi-MW electric motors while the inboard propellers are driven by conventional turboprops rated at 4,465 hp (~3.33 MW) per engine.

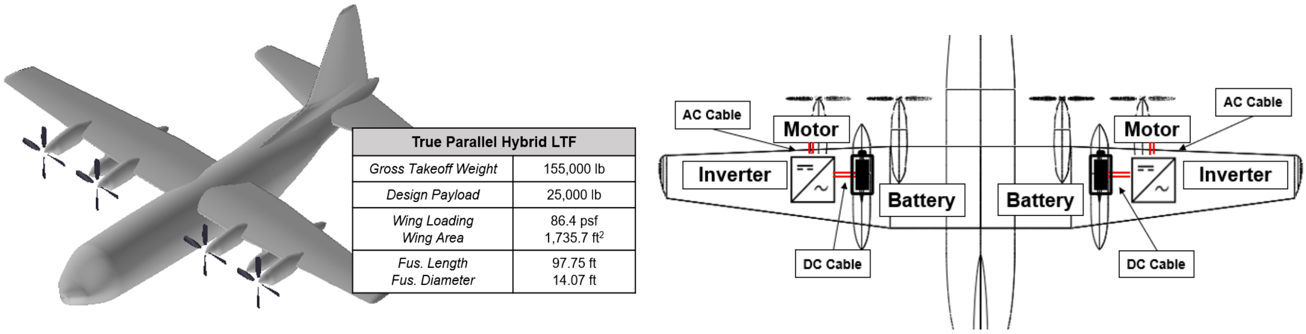

Figure 2. Configuration overview of the TPH LTF concept

Figure 2 depicts the high-level schematic of the TPH LTF concept where the primary components in this system include batteries, inverters, power distribution (shown as the AC and DC cabling), and motors. Thermal management systems (TMS) are included in the configuration and implemented as part of the EAP system weight and sized as a function of the peak electric power. Near-term EAP technologies will be studied using the TPH LTF concept that allow the overall configuration to close with benefits described parametrically using specific power and component efficiencies.

Table 1. Near-term EAP technology levels in terms of specific power and efficiency

	Specific Power				Efficiency			
	Min.	**Nom.**	**Max.**	**Unit**	**Min.**	**Nom.**	**Max.**	**Unit**
Battery	250	300	400	W-hr/kg	95%	98.5%	99.5%	%
Motor	5	10	15	kW/kg	92%	94%	95%	%
	1.65	1.91	3.33	MW				
Inverter	8	12	20	kW/kg	97%	99%	99.5%	%
Cabling	5.2	3.9	3.4	kg/m/MW	0.08%	0.04%	0.02%	% loss/m

Table 1 provides the summarized ranges of the component-level parameters such as specific energy density, power, specific power and efficiency for the electrical components, based on Refs. [4, 10, 11] for a multi-MW EAP system. The battery efficiencies are estimated for Li-ion battery technologies based on characteristic power curves that are a function of discharge rate and current [12]. If discharged slowly (~1/32 C), the charge efficiency can be as high as 99.5%, but the energy efficiency is typically 98.5% or lower. In Ref. [12], the battery efficiency model is a function of charging C-rate, discharging C-rate, and a technology factor (F_{BATT}) to approximate solid-state lithium (SSL) battery technology:

$$\eta_{BATT} = (1 - 0.0612x + 0.0115x^2 - 0.0781y + 0.0007873xy + 0.0124y^2)^{F_{BATT}} \quad (1)$$

In Equation (1), F_{BATT} = 0.19 to approximate SSL technology for this study where the curves were calibrated to 1.5C, x is the charging C-rate, y is the discharging C-rate, and η_{BATT} is limited to 1.0. The lower limit for and maximum electrical horsepower (EHPMAX) was determined by FAR Part 25.119-121 one-engine-inoperative (OEI) requirements for four-engine aircraft to achieve the required 3% climb gradient for 2nd segment OEI climb. For the TPH LTF configuration, the minimum EHPMAX that satisfied the 2nd segment OEI climb requirement was determined to be 1.645 MW (per motor). This achieved a climb gradient of 3.03%.

3. Modeling and Simulation (M&S) Overview

3.1 Tool Description & Sizing Methodology

Conceptual design and analysis of EAP concepts requires a highly integrated process that captures the dependences between the energy storage system, component-level powertrain performance, and power management throughout the mission profile. This is accomplished through integration of aircraft and EAP system sizing tools in a compact methodology that allows for design space exploration through variation of the component-level inputs, which is captured in the high-level design structure matrix in Figure 3, which was generated using the pyXDSM package [13].

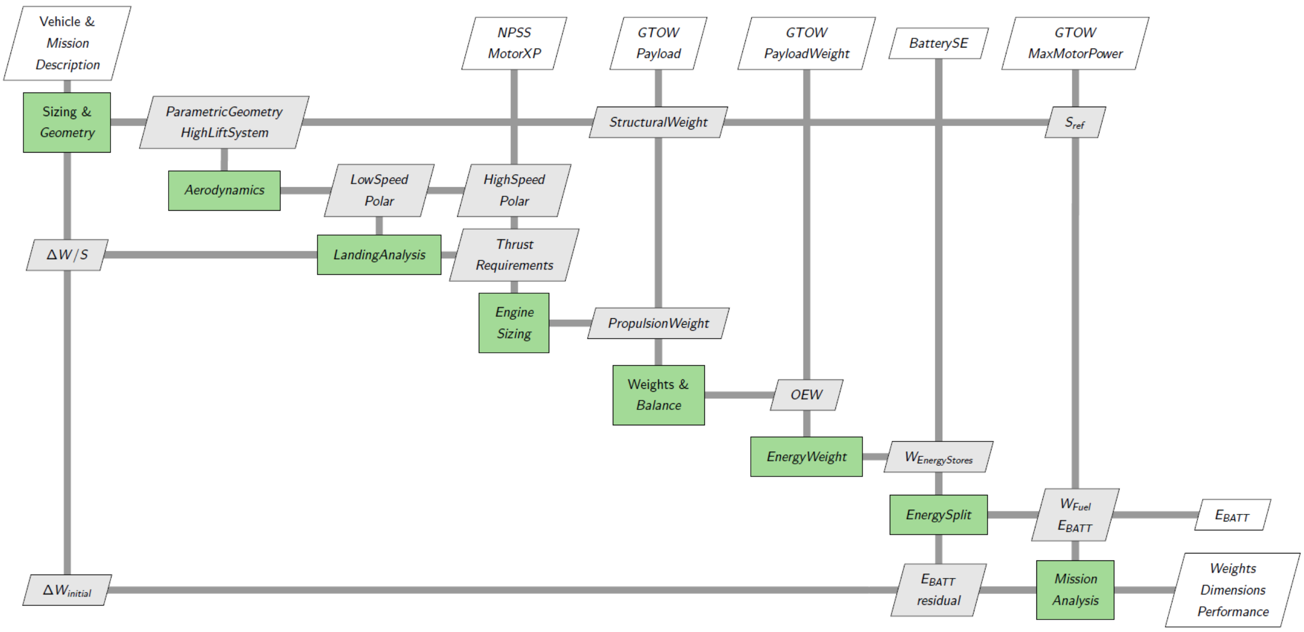

Figure 3. Design structure matrix for the integrated M&S environment

Figure 3 illustrates the extended design structure matrix for the integrated TPH LTF assessment. Given the airframe and propulsion configuration, mission performance requirements, and design mission specifications, the vehicle-level performance can be determined at each stage of the mission profile. Parametric modeling and aircraft sizing was done using the General Aviation Synthesis Program (GASP), a FORTRAN-based aircraft synthesis and mission analysis code developed at NASA Ames Research Center [14]. Under the EPFD project, GASP has been further developed to facilitate mission analysis of parallel hybrid turboprop configurations with methodology to account for sizing of hybrid fuel and battery systems [15]. GASP is initialized with parametric inputs that define the vehicle and mission specifications with two options for analysis: either the gross takeoff weight (W_{GTO}) is fixed and GASP outputs the fallout range as a single pass run, or a desired range is input, and GASP will iterate to determine the W_{GTO} [14]. For the conventional powertrain system, the baseline propulsion system model was calibrated to meet the LTF concept power requirements in the Numerical Propulsion System Simulation (NPSS) tool in a similar fashion to previous studies [5, 16]. To generate motor performance curves for the EAP system sizing analysis, the software MotorXP was used to obtain the torque-speed curves and efficiency maps [17]. The EAP component models were based on determining the weight penalties as a function of the specific power and EHPMAX is equivalent to the maximum motor output.

$$W_{component} = f\left(SP_{component}, EHPMAX\right) \tag{2}$$

Equation (2) represents the individual weight for each electrical component as a function of the specific power and EHPMAX, which is approximately a total of 3.82 MW (dual-sided) for the nominal TPH LTF configuration. The total weight contribution of an EPU can be determined as a sum of its constituents:

$$W_{EPU} = W_{BATT} + W_{CABLE} + W_{MOTOR} + W_{GBX,e} + W_{INVERTER} + W_{TMS} \tag{3}$$

Equation (3) shows that the sum of a single EPU includes the battery, cabling, motor, electric gearbox, inverter, and thermal management systems. In this study, gearbox technology is assumed constant, while TMS weight penalty is a function of EHPMAX. Since the TPH LTF features a dual-sided configuration, the EAP system contains two EPUs. The electrical component efficiencies impact the battery energy (E_{BATT}) and, thus, the fuel energy used at each flight phase:

$$E_{BATT_{phase}} = P_{TOTAL_{phase}}\left(t_{phase}\eta_{EPU}\right)\eta_{PROP} \tag{4}$$

$$\eta_{EPU} = \eta_{MOTOR}\eta_{GBX}\eta_{CABLE}\eta_{BATT}\eta_{INV} \tag{5}$$

Equations (4) and (5) are factored into the fuel usage, energy usage, electric system run time, and range performance in GASP, which considers the overall EAP system efficiency for all phases of flight. Here $\dot{m}$ is used to represent the fuel burn rate per engine, $e_{Jet\ A}$ is the specific energy of Jet-A, and $BSFC$ is the Brake Specific Fuel Consumption of a turboshaft engine.

$$\eta_{turbine_{cruise}} = \frac{HP_{shaft_{cruise}}}{\dot{m}_{cruise}*e_{Jet\ A}} = \frac{1}{BSFC*e_{Jet-A}} \tag{6}$$

Using Equations (5) and (6), an efficiency from onboard energy source to propeller shaft can be calculated and compared for both the EAP system and the conventional turboprop. For the EAP sizing methodology, the vehicle-level range performance is a fallout of the battery sizing module. To initialize the process, the gross takeoff weight, payload weight (W_{PL}), and battery specific energy density (SE_{BATT}) are input, where the battery weight (W_{BATT}) is either selected or sized. For parallel hybrid aircraft, the battery weight is added to the empty weight, but to find the available/required fuel weights, the operating empty weight without the EAP weight is used (W_{OEW}'). The fuel available is then computed as:

$$W_{F,available} = W_{GTO} – W_{OEW}' – W_{PL} – 2*W_{EPU} \tag{7}$$

Equation (7) shows how the available budget for fuel and electric energy storage ($W_{EnergyStores}$) is calculated, which is the sum of the battery weight and the fuel weight available. The mission is flown to consume all the available fuel, and the battery energy required is obtained by integrating the electrical power used during the mission. Initially, the energy split between the battery and fuel is estimated, with 85% of the available energy mass allocated to the battery and 15% to the fuel. This initial estimate is used to calculate an initial value of the battery energy available (E_{BATT}) and the residual battery energy ($E_{BATT,resid}$):

$$E_{BATT,resid} = E_{BATT} – E_{BATT,req} \tag{8}$$

Equation (8) computes the residuals in terms of the available battery energy and the required battery energy calculated in GASP. The energy-split is then iteratively adjusted to drive the residuals to zero, ensuring the energy allocation is balanced to deplete both stores by the end of the mission. The weight iteration process uses Newton-Raphson methods with underrelaxation to minimize the residual battery energy. This process can be written as:

$$E_{BATT,new} = \alpha E_{BATT,guess} E_{BATT} \left(\frac{d(E_{BATT,resid})}{d(E_{BATT})}\right)^{-1} \tag{9}$$

Equation (9) outlines this process where α is the underrelaxation factor ($0 < \alpha < 1$) and $d(E_{BATT,resid})/d(E_{BATT})$ is the derivative of the battery energy residuals with respect to the available battery energy. The value of α is set to 0.8 to stabilize the convergence process and control the step-size. The iteration process continues until the convergence criteria is achieved by minimizing the residuals to zero. Vehicle closure is achieved when the available fuel and battery energy match their required values computed by GASP, with the maximum range being a direct outcome of the battery sizing methodology.

3.2 Uncertainty Propagation

Aircraft performance assessment at the conceptual design phase inherently propagates uncertainties due to the variability in the design. Specifically, the integration of the MW-class EAP system comprised of novel electrical components introduces uncertain parameters, as many of these technologies are still in development, have unknown isolated and aggregated impacts, and have possible losses due to heat and performance degradation [4, 5]. The variations in component-level parameters such as mass, power, and efficiency impact overall vehicle performance metrics and must be captured stochastically, rather than deterministically. Therefore, Monte Carlo (MC) sampling and simulation is used with GASP with methods described in Ref. [16] to sample the input distribution of the component-level parameters based on the values in Table 1, obtain the performance distributions for high-level key metrics, and allow for exploration of EAP technology sensitivities. In this study, a Program

Evaluation and Review Technique (PERT) distribution is used to model the variability of the specific power and efficiencies of the electrical component by incorporating the minimum, maximum, and nominal estimates into a smooth, continuous curve resembling a β-distribution. Using the distributions described in Table 1, a MC analysis with 1,000 cases for each of the components was conducted, shown in Figure 4.

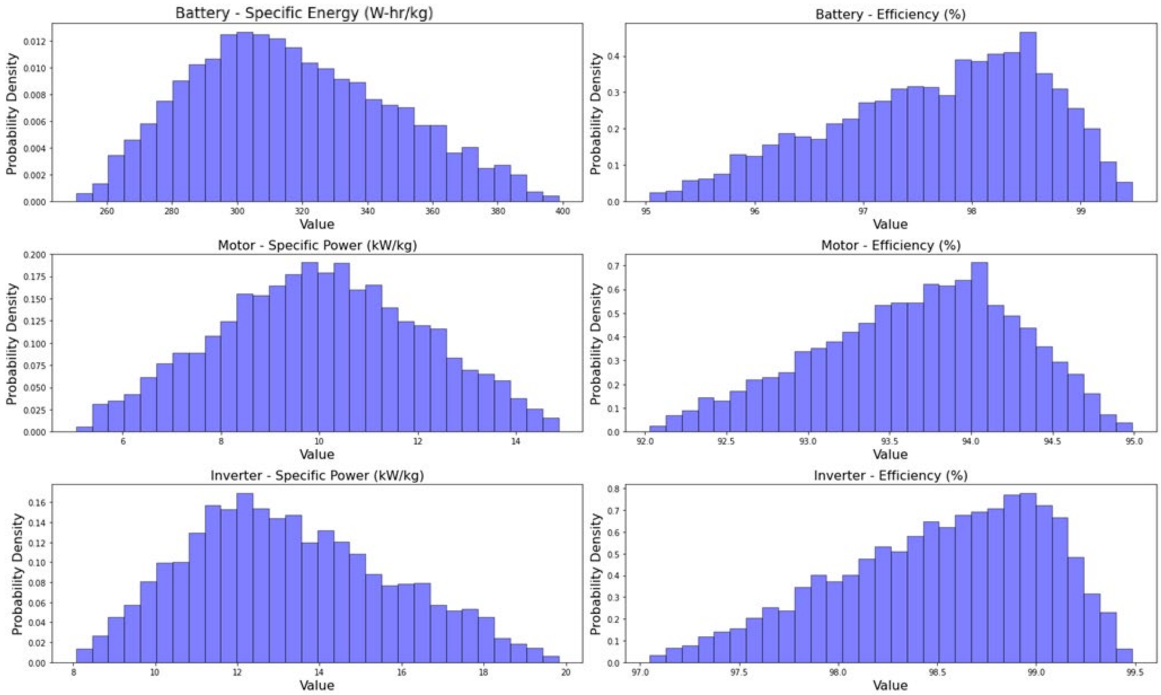

Figure 4. Probability distribution functions for the battery, motor, and inverter technology levels

3.3 Hybrid-Electric Mission Profile and Key Modeling Assumptions

To conduct a vehicle-level benefit assessment that captures the sensitivities to performance due to electrification, both baseline (LTF) and hybridized vehicle concepts (TPH LTF) were synthesized in GASP. The powertrain system is sized to meet the performance requirements at each stage of flight. The baseline LTF design payload-range mission for notional turboprop cargo aircraft was used to determine the energy requirements for taxi, All Engine Operating (AEO) and One Engine Inoperative (OEI) takeoff, top-of-climb rate of climb, 2nd Segment OEI climb gradient, and descent similar to Ref. [15]. This informed the hybrid-electric mission profile concept of operations.

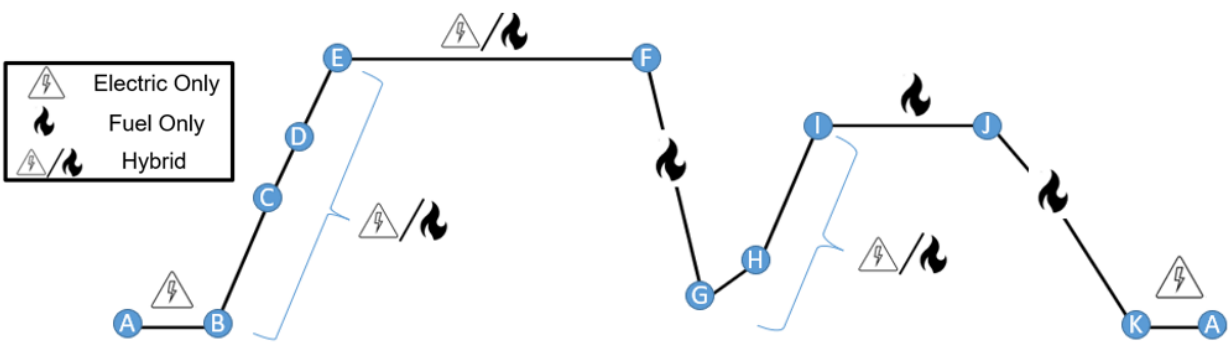

Figure 5. Notional hybrid-electric mission profile for the TPH LTF study

Figure 5 depicts the mission profile used for the notional TPH LTF vehicle, where a state-of-charge

(SOC) limit of 20% minimum was imposed:

A. **Taxi In/Out:** When operating as a parallel hybrid vehicle, the TPH LTF will utilize electric energy only to power the motors for taxiing in and out (4.5 minutes), referred to as electric taxi (E-taxi) in Ref. [18]. Typically, this is done at idle setting for the conventional turboprop, though gas turbine efficiency at idle is significantly less than for electric machines.
B. **Takeoff:** Both electric and conventional gas turbine power systems are at maximum takeoff power settings – field length will vary based on EHPMAX.
C. **Acceleration I:** Both propulsion systems are at maximum takeoff power settings for acceleration to best rate-of-climb speed (V_Y) which is ~180 KEAS.
D. **Climb:** Both propulsion systems are set to maximum climb power (MCP) setting to maintain V_Y – climb performance will vary based on EHPMAX. Acceleration II occurs at the end of climb to the cruise speed and altitude.
E. **Cruise:** Both propulsion systems are providing thrust through the cruise segment, done at a constant altitude of 21,000 ft at Mach 0.475 where the power split for the EAP system is determined by EHPMAX.
F. **Descent:** Only using the conventional gas turbine power systems at idle power with the EPUs set to windmilling configuration. Option for battery charging during descent.
G. **Missed Approach*:** Is the start of the reserve mission profile and utilizes both power systems to climb to reserve cruise altitude.
H. **Reserve Climb*:** Both propulsion systems are set to MCP to reserve altitude of 10,000 ft.
I. **Reserve Cruise*:** Only using the conventional gas turbine power systems at normal rated power for the 100 NM cruise to an alternate airport to avoid significant battery weight penalty/charge depletion during the reserve mission.
J. **Reserve Descent/Hold Time*:** Same as F, except with 30-minute hold time at 1,500 ft altitude.
K. **Landing:** For sizing, percent landing weight is set to 97.6% and performed only using the conventional gas turbine power systems at idle power. At landing, the charge should be no less than the 20% minimum SOC limit.

Cruise is performed at constant altitude of 21,000 ft at Mach 0.475, where the power split for the EAP system is determined by which cruise mode of operation is selected. Instead of thrust-split optimization, this study employs the methodology of fitting operational profiles based on running either the electric or conventional powertrain systems at 100% normal rated power (NRP) and making up the difference in required thrust with the alternate power system. Required thrust for cruise is determined for steady, equilibrium cruise flight:

$$D = \frac{1}{2}\rho V^2 S_{REF} C_D = T \tag{10}$$

Equation (10) finds the thrust required (T) in pounds-force, which is approximately 9,250 lbf. This is the same thrust requirement for cruise for the TPH configuration, where the thrust is provided by the motor and turbine.

$$T_{TPH} = T_{MOTOR} + T_{TURBINE} \tag{11}$$

Equation (11) defines the thrust for the TPH which is a contribution of the thrust from the electric motors and gas turbine propulsion systems. The thrust-split is the ratio of the total thrust from the motor-driven propellers over the total thrust from the combined propulsion system, where either the motor or turbine is selected to run at NRP. For this study, the motor is run at NRP during cruise, with the turbines making up the difference, which evaluates the highest potential fuel savings. The alternative study would optimize for improved range performance with reduced fuel savings [15].

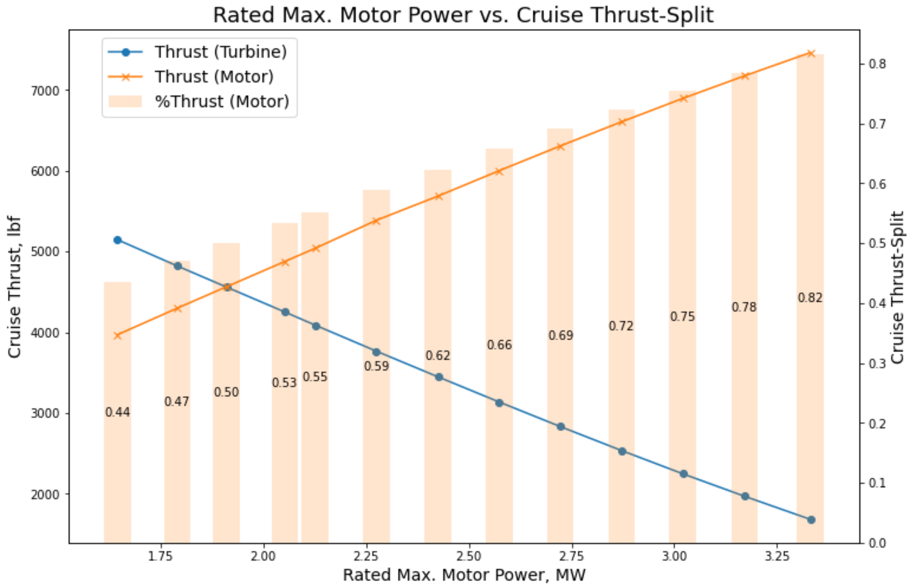

Figure 6. Cruise thrust-split as a function of the rated maximum motor power (per motor) for the TPH LTF concept

Figure 6 presents the cruise thrust-split between the gas turbines and electric motors for nominal inverter, cabling, TMS, and battery technology levels as a function of the maximum rated motor power per EPU. With increased maximum motor power required from the EAP system, the thrust contribution from the motor increases with less thrust required for the gas turbine-driven propellers. A crossover point at 1.910 MW per motor (~2,560 shp) is where the thrust from the motors is equivalent to the thrust from the gas turbines; past this point, the electric motors provide the bulk of the cruise thrust. Prior to design space exploration, preliminary sizing studies were conducted to determine the EAP technology levels required to meet the power requirements of the TPH LTF concept. Models for the conventional gas turbine, electric propulsion system, and propeller performance were provided to GASP as lookup tables in the propulsion module. The standard-day, sea-level static takeoff rating in NPSS was 4,465 propeller shaft horsepower, where the reference gear ratio is calculated assuming the given values for the constant turbine and shaft speed.

Table 2. Propulsion system characteristics for the TPH LTF concept

Engine Parameter	**Value**		**Propeller Parameter**	**Value**
SLS Takeoff Rating, shp	4,465		Activity Factor	162
SLS TO Tailpipe Thrust, lbf	800		Propeller Diameter, ft	13.5
Reference Gear Ratio	0.0738		Maximum Allowable Tip Speed, ft/s	720
Ambient Conditions	ISA		Number of Blades	4
Constant Turbine Speed, RPM	13,820		Model	Hamilton Standard
Constant Shaft Speed, RPM	1,020		Integrated Lift Coeff.	0.5

Electric Motor Parameter (Per Motor)	**Value**
Base Speed, RPM	1,350
Max. Torque, N-m	22,500
Max. Input Power, MW	3.33
Max. Current, A-rms	1,964
Percent Power @ NRP, %	92.8

Table 2 depicts the propulsion system specifications for the conventional turboprop modeled in NPSS [19], the Hamilton Standard propeller model used within GASP, and the multi-MW electric motor design created in MotorXP [17]. The propeller parameters are used to initialize the Hamilton Standard propeller performance sub-routine in GASP, where the thrust coefficient and propeller efficiency is determined as a function of the propeller activity factor, diameter, number of blades, and shaft horsepower [20]. For this study, the propeller design for the TPH LTF configuration is the same as the baseline LTF, with a fixed diameter and number of blades. To model the EAP system, additional parametric inputs related to the multi-MW motor were required to define the motor performance model in Motor XP including maximum horsepower, design motor RPM, gear ratio, reference motor efficiency, and maximum continuous specific horsepower.

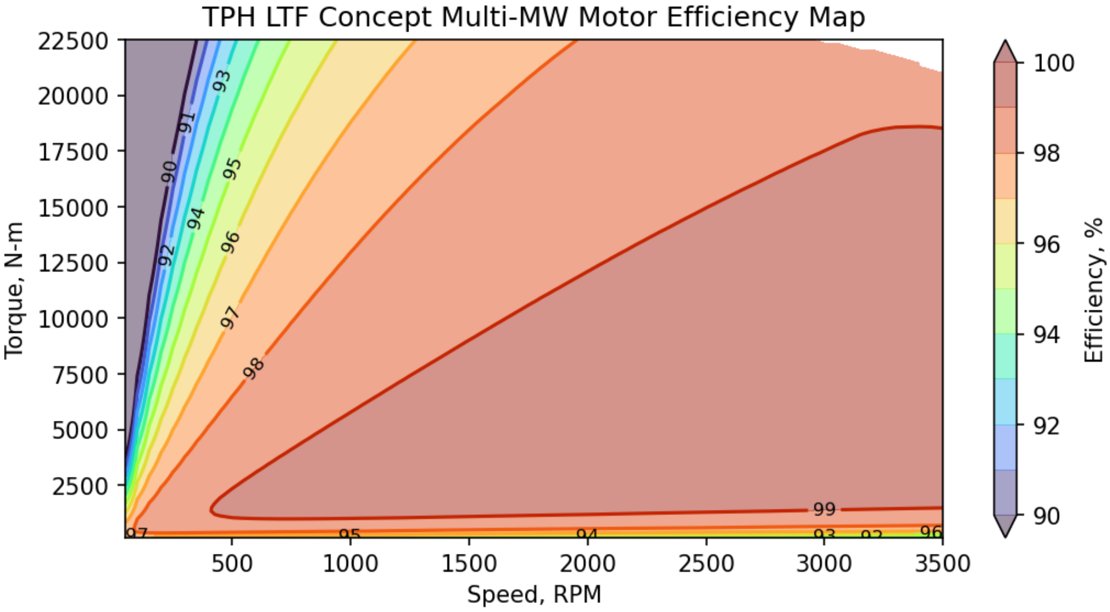

Figure 7. MW-class motor efficiency map used for TPH LTF concept models

Figure 7 depicts the composite contour plot of the motor efficiencies at given torque-speed operating points for the multi-MW motor used in this study. The maximum torque was set at 22,500 N-m with a maximum input power of 3.32 MW, which can be scaled to the specified maximum electrical system horsepower in GASP. The normal rated power motor performance was determined by the maximum continuous specific horsepower at 50% de-rated torque. While the motor efficiency is related to the motor RPM derived from the motor model, a motor technology factor is used to adjust the RPM accordingly to obtain the desired motor efficiency values to match Table 1. The maximum torque limit is determined by the magnitude of the current directed to the motor, while the motor speed is based on the voltage frequency. In this case, it was assumed the motor had a variable frequency drive.

Once the conventional gas turbine and electrified propulsion systems were parametrically modeled and established in the propulsion module, the vehicle-level configuration models and mission analysis could be initiated. The analysis was conducted with the fixed geometry inputs shown in Figure 2 where both the baseline LTF and hybrid electric TPH LTF vehicle models were initialized with a maximum gross takeoff weight of 150,000 lb, a design payload of 25,000 lb, vehicle structural weight of approximately 45,000 lb, and takeoff wing loading of 86.4 psf. The remaining weight budget was then allocated to the propulsion and energy storage systems. Battery weight was fixed at 42,000 lb for all TPH LTF configurations. The outboard propulsors of the baseline LTF were replaced with the multi-MW EPUs and infused with the nominal EAP component-level performance specifications from Table 1 to observe the impacts of hybrid electrification.

Table 3. Baseline LTF and TPH LTF given nominal EAP technology levels

Performance Parameter	Baseline LTF	TPH LTF (Nominal)	Δ%
Gross Takeoff Weight (GTOW), lb	150,000	150,000	-
Operating Empty Weight (OEW), lb	80,000	116,200	+45.3
Design Payload (W_{PL}), lb	25,000	25,000	-
Max. Payload ($W_{PL,max}$), lb	42,000	26,810	-36.2
Design Range for W_{PL}, NM	2,528	314	-87.6
Loaded Fuel for Design W_{PL} (WFA), lb **Battery Capacity, kW-hrs**	45,000 0	8,800 5,715.4	-80.4 -
Block Fuel Used for 300 NM mission, lb	5,622	3,220	-42.7
Number of Engines, # **Turbine** **Motor**	 4 0	 2 2	 - -
Max. Rated Power, hp **Turbine** **Motor**	 4,465 0	 4,465 2,560	 - -
Takeoff T/W, hp/lb **Turbine** **Motor**	 0.2458 0	 0.1229 0.1020	 -50 -
AEO Takeoff Field Length, ft	4,445	5,310	+19.5
OEI Takeoff Field Length, ft	4,832	6,315	+30.7
2nd Segment OEI Rate-of-Climb, fpm	1,050	512	-51.2
Top-of-Climb Rate-of-Climb, fpm	1,238	814	-34.3
BSFC, lb/hr/lb	0.5678	0.5695	+0.3
Specific Range, NM/lb	0.07502	0.12955	+72.7

Table 3 provides a vehicle-level performance summary of the baseline LTF and TPH LTF infused with the "nominal" component-level specifications from Table 1. The nominal configuration is where the EHPMAX is 2,560 hp (1.645 MW) per motor, where the total cruise thrust is split equally between the conventional turboprops and EPUs, as shown in Figure 6. Since EHPMAX is less than the total rated power of the conventional turboprops and the increased weight from the EAP system, the AEO and OEI takeoff field length increases for the TPH LTF, with lower rate-of-climb values. As expected, the OEW is increased for the TPH LTF because it includes the added EAP system weight, where the battery weight is the most significant contributor. For a 300 NM mission, the nominal TPH LTF configuration results in 42.7% block fuel savings, though hybridization results in reduced payload capacity and range performance.

4. Results

Component-level EAP technology sensitivity studies and energy profiling was conducted for the TPH LTF concept for missions flown with the motor at NRP during cruise and with a 25,000 lbf payload. To account for differences in closed mission range and the combination of energy sources, all aircraft will be compared using their Energy Consumption per Nautical Mile (ECNM). The conventional LTF, that runs exclusively on Jet-A, had an ECNM of approximately 90.9 kWh/nm. The range capabilities for the TPH LTF aircraft when cruising with the electric motor at NRP were limited to 100 to 300 NM, as the study focused on near-term, 2030 to 2035 EAP technology levels. The TPH configurations utilized less energy, as the EAP system was capable a of higher conversion efficiency of 91.3% compared to the conventional Jet-A propulsive efficiency of 29.9%.

Table 4. EAP component-level breakdown in ECNM reduction

	5th Percentile	25th Percentile	Median	75th Percentile	95th Percentile
Battery	22.3%	23.8%	25.0%	26.2%	27.4%
Motor	23.8%	24.3%	24.5%	24.7%	24.9%
Inverter	24.0%	24.3%	24.5%	24.7%	24.8%
Cabling	24.2%	24.4%	24.6%	24.7%	24.8%
TMS	24.7%	24.7%	24.7%	24.7%	24.7%
Overall	21.4%	23.2%	24.5%	25.6%	26.9%

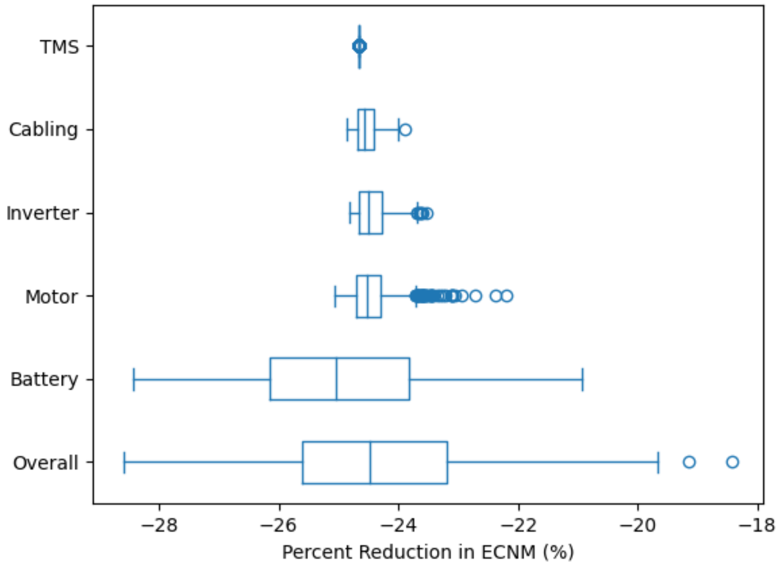

Figure 8. Distribution of EAP component-level breakdown of ECNM savings

Table 4 illustrates the high-level ECNM reduction based on the results of the MC analysis, and Figure 8 presents the box-and-whisker plot of the resulting distributions. As observed, the EAP system component with the greatest impact on energy consumption is the battery, particularly in terms of specific energy density and efficiency. The specific energy density of the battery was a critical factor in achieving vehicle closure, with the minimum required specific energy density, SE_{BATT} being approximately 200 Wh/kg for the TPH LTF, given the design mission profile. This value is close to the current state-of-the-art battery technology, which is approximately 250 Wh/kg. In terms of vehicle-level performance sensitivities, the battery exhibited the most significant impact and variability in ECNM reduction, with percentiles ranging from 22.3% to 27.4%. These results suggest that improvements in battery technology have the greatest potential to influence vehicle-level performance sensitivities for the multi-MW TPH LTF concept.

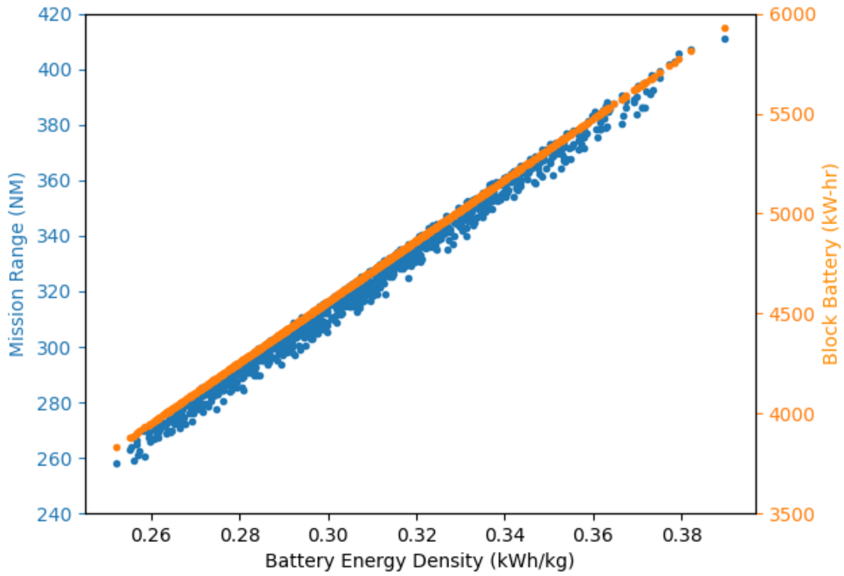

Figure 9. Sensitivity analysis of battery specific energy density on range performance and block battery energy consumption (1,000 MC cases)

Figure 9 shows the results of the focused sensitivity study where battery energy density was varied. For a fixed battery weight, increasing the battery energy density results in higher battery capacity. There is a strong correlation between battery energy density and maximum range. Consequently, the block battery energy available for the mission increases (considering a 20% minimum SOC limit), leading to an improvement in the overall mission range and greater fuel savings.

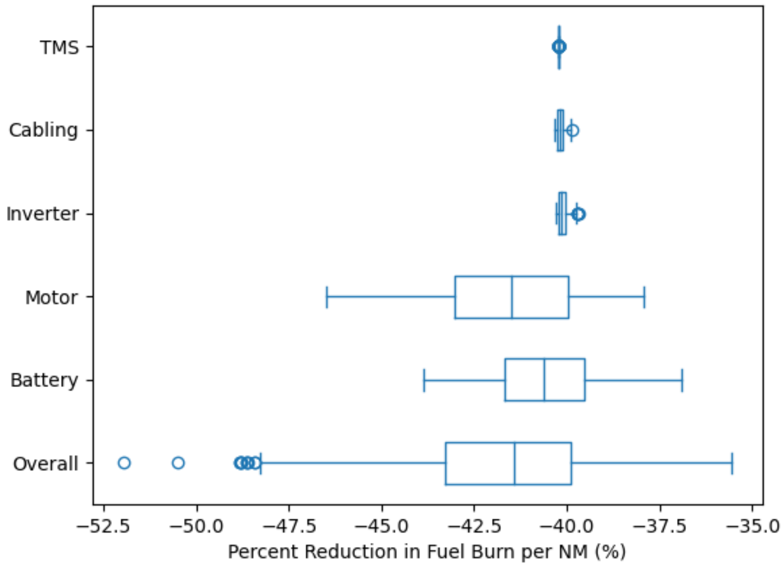

Figure 10. EAP component-level breakdown of fuel burn per nautical mile percent reduction

Figure 10 shows the fuel burn per nautical mile reduction as a function of the component-level specific power and efficiencies for the multi-MW EAP system. Similarly to Figure 8, the largest contributor to vehicle-level performance benefits in improved fuel efficiency per nautical mile is the battery, where the key metric is SE_{BATT}. For this study, increasing the TMS weight from 384 lbs. to 640 lbs. constituted a change of less than 0.2% of the total vehicle weight, and resulted in negligible impact on the vehicle performance. Even though a low fidelity model of the TMS weight estimation was used, increasing the fidelity of the weight model will have little effect on reducing the overall uncertainty. However, better modeling of the impact the TMS has on the efficiency of the motor, inverter, and battery could provide moderate reductions in the overall uncertainty. While the range performance had little sensitivity to the motor specific weight variations, motor efficiency had a small, but noticeable impact on the vehicle-level range performance.

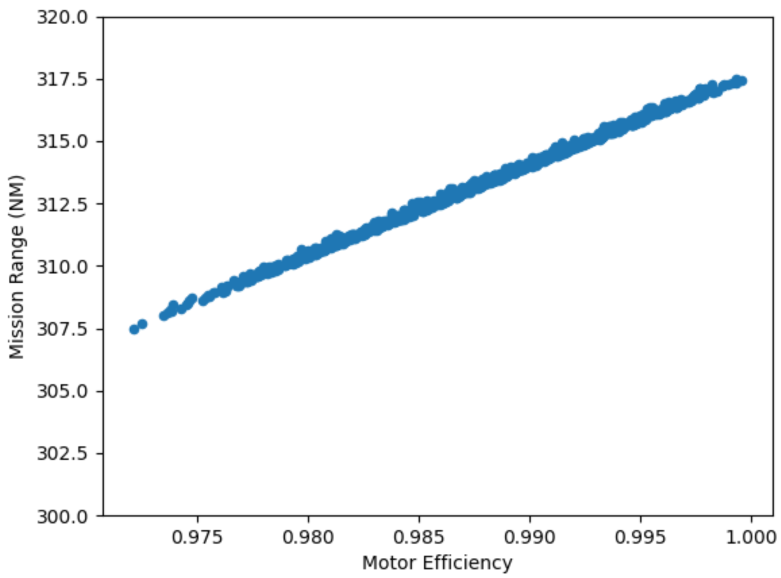

Figure 11. Sensitivity analysis of motor efficiency on range performance and block battery energy consumption for the nominal motor (1,000 MC cases)

Figure 11 depicts the mission range as a function of the motor efficiency where all other non-motor EAP technology levels were fixed at the nominal values, showing strong correlation between motor efficiency and range improvement. The full impact of motor performance is best captured by profiling the energy and fuel consumption for each phase of the mission profile. This involves detailing TPH LTF configurations that demonstrate minimum, nominal, and maximum assumed EAP technology levels, where the overall peak power of the electrical propulsion system is gradually augmented. Block fuel weight (BF) and block battery energy (BE) values were determined for each flight phase across the representative TPH LTF configurations, where block fuel savings per phase (-ΔBF, relative to the baseline LTF) was reported for a 300 NM mission range.

Table 7. Block fuel burn, energy consumption, and block fuel savings per mission phase for the minimum, nominal, and maximum EAP system technology levels (300 NM mission)

Flight Phase	LTF (Base)	TPH LTF (Min.)			TPH LTF (Nom.)			TPH LTF (Max.)		
	BF, lb	BF, lb	BE, kW-hr	-ΔBF, %	BF, lb	BE, kW-hr	-ΔBF, %	BF, lb	BE, kW-hr	-ΔBF, %
Taxi	622	0	143.6	100	0	129.4	100	0	126	100
Takeoff	135	87	69.4	35.6	83	69.4	38.5	72	102	46.7
Accel.	66	55	45	16.7	50	43	24.2	34	49	48.5
Climb	1,691	1,406	1,344	16.9	1,277	1,273	24.5	882	1474	47.8
Cruise	2,297	1,574	1,709	31.5	1,488	2,517	35.2	745	3,543	67.5
Descent	811	152	0	81.3	322	0	60.3	333	0	58.9
Reserve	6,791	3,754	619.6	44.7	3,772	602.7	44.5	3,662	816.6	46.1
Total Mission*	5,622	3,274	3,311	41.8	3,220	4,032	42.7	2,066	5,294	63.3

**Reserves not included in mission totals*

Table 7 presents the block fuel and energy usage per flight phase for the TPH LTF concept. Most noticeably, improved component efficiencies and specific powers result in reduced energy consumption for a given phase. For the baseline configuration, the taxi segment accounts for 11% of the total block fuel, where significant overall fuel savings can be achieved by E-Taxi for the TPH LTF configurations. Approximately 2.4-4.3% of the total block energy is required for E-Taxi, which results in reduced energy consumption because the gas turbine propulsion system is inefficient at idle power settings while electric transmission has greater propulsive efficiency. As most of the fuel consumption for the baseline LTF derives from climb (30%) and cruise (40.8%), higher power draw from the electric power system supplemented with increased total battery capacity to maintain those levels result in significant fuel savings ranging from 17-48% during climb and 32-68% during cruise. Improvements in EAP technologies, along with higher power draw from the electrical power systems, result in significant fuel savings for a 300 NM design range, with 40-63% fuel savings. When the EAP system EHPMAX was equivalent to the maximum rated power of the conventional turboprop system, the takeoff field length and rate of climb performance matched the baseline configuration, while simultaneously saving energy consumption during those phases. However, while the TPH LTF configuration with maximum EAP technology levels had the highest overall fuel savings for the same range, the maximum range performance was reduced.

5. Conclusions

This paper presented an approach to parametric modeling of MW-class EAP systems using a large turboprop freighter concept vehicle utilizing a true parallel hybrid electric propulsion architecture. The impact of MW-class EAP system integration on fuel savings, range performance, and energy consumption was studied using engineering-level, physics-based models and mission performance analyses in GASP, where an integrated battery sizing approach was implemented. The results provide a detailed breakdown of the contributions that component-level parameters have on the overall vehicle-level aircraft performance and fuel efficiency. Key drivers for overall vehicle performance improvements were identified as the battery specific energy density, maximum EAP system power output, and motor efficiency. Improving the battery specific energy density from 250 to 400 Wh/kg resulted in ~25% improvement in ECNM due to the improved transmission efficiency from EAP systems compared to conventional gas turbine propulsion systems and 40-63% fuel savings for a 300 NM mission. The results of this study indicate that increased EHPMAX contribute significantly to improved fuel efficiency per nautical mile, while enhancements in battery technology, particularly in specific energy density, drive notable improvements in ECNM. This study enables benchmarking of the progress of near-term EAP technology levels spanning from 2020 to 2035 by providing the electrical power requirements of a multi-MW, true parallel hybrid concept with a representative short-haul cargo mission. The minimum EAP system electric power requirements to meet the OEI climb gradient requirements for a four-engine aircraft, were determined to be 1.645 MW rated motors (dual-sided), highlighting potential vehicle-level design considerations for next-generation hybrid-electric aircraft configurations. Sensitivity analyses conducted for the TPH LTF concept show areas for targeted improvements for multi-MW EAP concepts; advancements in battery technology resulting in specific energy levels greater than 200 Wh/kg will be pivotal for optimizing vehicle range and energy consumption. At the same time, improvements in motor efficiency will result in improved propulsive efficiency and consequently better range performance. This study offers a pivotal evaluation of near-term EAP technology levels for integrating a multi-MW system within a true parallel hybrid large turboprop freighter concept, providing an integrated approach to sizing and capturing vehicle-level performance sensitivities to hybrid electric powertrain architecture metrics.

6. Contact Author Email Addresses

For questions concerning the paper please contact: dahlia.d.pham@nasa.gov and carl.recine@nasa.gov.

7. Copyright Issues

8. Acknowledgements

The research reported in this paper is funded by NASA's Electrified Powertrain Flight Demonstration (EPFD) project. The authors would like to acknowledge Gaudy Bezos-O'Connor, Andrew Meade, Kevin James, Susie Go, Jeffryes Chapman, Gregory Zilliac, Noah Listgarten, Jeffrey V. Bowles and Lee Kohlman for providing support for this project.

References

[1] International Civil Aviation Organization (ICAO), "Report on the feasibility of a long-term aspirational goal (LTAG) for international civil aviation CO2 emission reductions," in *ICAO Committee on Aviation Environmental Protection (CAEP)*, 2022.

[2] Haran, Kiruba, Madavan, Nateri, and O'Connell, Tim C., Electrified Aircraft Propulsion: Powering the Future of Transportation, Cambridge University Press, 2022.

[3] NASA Aeronautics Mission Directorate (ARMD), "Electrified Powertrain Flight Demonstration," 19 April 2022. [Online]. Available: https://www.nasa.gov/aeroresearch/programs/iasp/epfd.

[4] Haglage, Joseph M., Dever, Timothy P., Jansen, Ralph H., and Lewis, Maxwell A., "Electrical System Trade Study for SUSAN Electrofan Concept Vehicle," NASA Glenn Research Center, Cleveland, OH, 2021.

[5] Kirk, Jason T., Frederick, Zachary J., Guynn, Mark D., Phillips, Ben D., Fisher, K. L., Schneider, S. J., and Frederic, Peter, "Continued Exploration of the Electrified Aircraft Propulsion Design Space," in *AIAA SciTech Forum 2023*, National Harbor, MD, 2023.

[6] Borer, N. K., Patterson, M. D., Viken, J. K., Moore, M. D., Bevirt, J., Stoll, A. M., and Gibson, A. R., "Design and Performance of the NASA SCEPTOR Distributed Electric Propulsion Flight Demonstrator," in *AIAA Aviation Forum*, Washington D.C., 2016.

[7] Antcliff, K. R., and Capristan, F. M., "Conceptual Design of the Parallel Electric-Gas Architecture with Synergistic Utilization Scheme (PEGASUS) Concept," in *AIAA Aviation Forum*, Denver, CO, 2017.

[8] Cai, Y., Xie, J., and Mavris, D., "Advanced 2030 Turboprop Aircraft Modeling for the Electrified Powertrain Flight Demonstration program," in *AIAA SCITECH 2022 Forum*, Anaheim, CA, 2022.

[9] Cai, Y., Xie, J., Gladin, J. C., and Mavris, D., "System-Level Design Space Exploration of a Parallel Hybrid Propulsion System for a Regional Short Takeoff and Landing," in *AIAA Aviation Forum 2023*, San Diego, CA, 2023.

[10] Tiede, Blake, O'Meara, Cody, and Jansen, Ralph H., "Battery Key Performance Projections based on Historical Trends and Chemistries," in *IEEE Transportation Electrification Conference and Expo (ITEC)*, Anaheim, CA, 2022.

[11] Dever, Timothy P., Lantz, Terry J., and Jansen, Ralph H., "Cable Key Performance Parameter Projections for Megawatt Electrified Aircraft Propulsion Models," in *AIAA SciTech Forum*, Orlando, FL, 2024.

[12] Zilliac, Gregory G., Bowles, Jeffrey V., Fong, Robert K., Schuh, Michael J., Pham, Dahlia D. V., and Kuptsov, Vladimir, "Feasibility Study of an All-Electric 150 Passenger Aircraft," in *AIAA Aviation Forum*, Las Vegas, NV, 2024.

[13] Lambe, A. B., and Martins, J. R. R. A., "Extensions to the design structure matrix for the description of multidisciplinary design, analysis, and optimization processes," *Structural and Multidisciplinary Optimization,* vol. 46, no. 2, pp. 273-284, 2012.

[14] Hague, D., " GASP- General Aviation Synthesis Program," NASA Contractor Report , Bellevue, WA, 1981.

[15] Pham, Dahlia D. V., Bowles, Jeffrey V., Zilliac, Gregory G., Go, Susie, and Listgarten, Noah S., "Parametric Modeling and Mission Performance Analysis of a True Parallel Hybrid Turboprop Aircraft for Freighter Operations," in *AIAA Aviation Forum*, Las Vegas, NV, 2024.

[16] Pham, Dahlia D. V., Bowles, Jeffrey V., Recine, Carl, and Go, Susie, "Advanced Turboprop Transport Aircraft Modeling for the Electrified Powertrain Flight Demonstration Project," in *AIAA Aviation 2023 Forum*, San Diego, CA, 2023.

[17] MotorXP, "MotorXP: Electric Machine Design and Analysis Software," Vepco Technologies, Inc., 14 November 2023. [Online]. Available: https://motorxp.com/#motorpm. [Accessed 8 August 2022].

[18] Fredericks, Zachary J., Hallock, Thomas J., Ozoroski, Thomas A., Chapman, Jeffryes W., Kunle, Caroline A., and Frederic, Peter C., "Design Exploration of a Mild Hybrid Electrified Aircraft Propulsion Concept," in *AIAA Aviation Forum*, San Diego, CA, 2023.

[19] Lytle, J.K., "The numerical propulsion system simulation: An overview," NASA Glenn Research Center/ NASA TM-2000-209915, Cleveland, OH, 2000.

[20] Worobel, R., "Hamilton Standard Prop Code: Computer Program User’s Manual for Advanced General Aviation," NASA CR-2066, 1972.